Transition Radiation in Photonic Topological Crystals: Quasiresonant Excitation of Robust Edge States by a Moving Charge

Yang Yu,[1] Kueifu Lai,[2,1] Jiahang Shao,[3] John Power,[3] Manoel Conde,[3] Wanming Liu,[3] Scott Doran,[3] Chunguang Jing,[3] Eric Wisniewski,[3] and Gennady Shvets[1,*]

[1]*School of Applied and Engineering Physics, Cornell University, Ithaca, New York 14853, USA*
[2]*Department of Physics, University of Texas at Austin, Austin, Texas 78712, USA*
[3]*Argonne National Laboratory, Lemont, Illinois 60439, USA*

(Received 14 February 2019; published 31 July 2019)

We demonstrate, theoretically and experimentally, that a traveling electric charge passing from one photonic crystal into another generates edge waves—electromagnetic modes with frequencies inside the common photonic band gap localized at the interface—via a process of transition edge-wave radiation (TER). A simple and intuitive expression for the TER spectral density is derived and then applied to a specific structure: two interfacing photonic topological insulators with opposite spin-Chern indices. We show that TER breaks the time-reversal symmetry and enables valley- and spin-polarized generation of topologically protected edge waves propagating in one or both directions along the interface. Experimental measurements at the Argonne Wakefield Accelerator Facility are consistent with the excitation and localization of the edge waves. The concept of TER paves the way for novel particle accelerators and detectors.

DOI: 10.1103/PhysRevLett.123.057402

Generation of electromagnetic (EM) waves by moving electric charges is one of the most fundamental phenomena in physics. While a charge must be accelerated to produce EM radiation in free space, this requirement no longer exists in optically dense media. Even in a homogeneous isotropic medium, the Cherenkov radiation (CR) [1] by a charge traveling with a constant velocity v can be produced when the phase velocity v_{ph} of EM waves is smaller than v. In an inhomogeneous medium, transition radiation (TR) [2] —usually studied in the context of a charge crossing an interface between two media with different permittivities and/or permeabilities—can also be produced by a constant-velocity motion [3–10] regardless of the magnitude of v. TR has already found numerous applications in particle detectors and beam diagnostics [9,11]. More recently, there has been considerable interest in expanding the TR concept to more complex geometries and structures, including the resonant transition radiation [12–15] in multi-interfacial materials that form a one-dimensional (1D) photonic crystal. TR has also been used to excite surface plasmon polaritons (SPPs) [6,16] and guided modes in thin films [17,18], which are hard to be directly excited by far-field (e.g., laser) radiation.

The key limitation of all these approaches to producing TR is that fast charged particles must be sent through a solid medium, resulting in rapid energy loss by the electrons, as well as the inevitable incoherent emission [19]. For example, a 1 MeV electron loses all of its energy after propagating through just under 3 mm of silicon. Charging of multilayer dielectric structures bombarded by high-charge bunches also limits their longevity [20]. Therefore, one is led to consider an intriguing yet unexplored possibility of producing TR in a photonic crystal (PHC) designed to have an empty region that provides an unobstructed path for the moving charge (see Fig. 1). However, the physics of TR excitation in two- and three-dimensional periodic media has not been studied either theoretically or experimentally, with a few exception of 1D multilayer films [12,14,15]. Even in those studies, the emphasis was on the excitation of the modified Cherenkov (i.e., bulk) radiation, and the feasibility of sending electrons through solid medium was assumed. In this Letter, we extend the concept of TR to the case of a charge crossing the interface between two PHCs and emitting *guided waves* that are localized to the interface. In particular, we consider the previously unexplored concept of TR into topologically protected edge waves (TPEWs) that exist at the domain wall between two topologically distinct photonic topological insulators (PTIs) [21–24]. We demonstrate that the moving charge breaks the time-reversal symmetry of TPEWs and enables spin- and valley-polarized emission of TPEWs that are routed into spin-locked ports. In condensed matter physics it has been shown that circularly polarized light can excite spin-locked currents on the surface of topological insulators [25]. Among practical attractions of TPEWs are their one-dimensional (i.e., localized in the other two dimensions) nature, and the ability for reflection-free propagation around sharp corners [26]. Similarly to SPPs, TPEWs cannot directly couple to bulk EM waves. However, SPPs can be also excited by

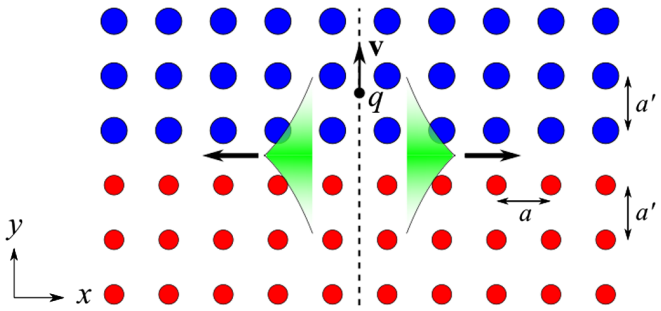

FIG. 1. A schematic of transition radiation by a point charge at the interface of two photonic crystals. The charge moves from one PHC (small, red circles) to another (large, blue circles) with constant velocity v. Guided (edge) modes (green shades) propagating in the x direction are excited with frequencies inside the shared band gap of the two PHCs, as well as bulk modes (not shown) at frequencies outside the band gap. The period a along x direction and the lattice period a' along the beam's path are labeled.

moving charges via the CR mechanism [19] because their dispersion curves are below the light line ($v_{\mathrm{ph}} < c$) due to their polaritonic nature, while TPEWs frequently cannot be because the phase velocities of the guided EM waves typically satisfy $v_{\mathrm{ph}} > c$.

We start by developing a general formalism of guided waves' excitation by a TR mechanism as illustrated in Fig. 1, where a point electrical charge q is shown moving uniformly with velocity v, crossing the boundary at $y = 0$ between two different PHCs sharing the same crystal lattice, and exciting two counterpropagating edge states. Alternative configurations are described in Supplemental Material [27], including the excitation of guided modes of a linear defect inside a PHC. For simplicity, we focus on two-dimensional (2D) PHCs that do not rely on a photonic band gap (PBG) for their confinement in the z dimension, but most of the results can be generalized to 3D. We further assume that the PhCs are non-magnetic and lossless.

Because the structure is still periodic in the x (albeit not in the y) direction, we choose an expanded "supercell" of the photonic structure comprised of one unit cell (of either PHC) in x and infinitely many in y direction. The supercell is used to compute the 1D Bloch states $\mathbf{E}_{k,n}(\mathbf{r}) = \mathbf{u}_n(k,\mathbf{r})\exp(ikx)$, where the supercell's normalized x-periodic eigenmodes $\mathbf{u}$ are characterized by their band number n, wave number k along the interface, and eigenfrequency $\omega_n(k)$. The eigenmodes can be subdivided into two classes: (i) projected [33] bulk (extended) modes that have oscillatory behavior in y, and (ii) edge modes that exponentially decay as $e^{-\kappa|y|}$ away from the domain wall at $y = 0$, where $\kappa^{-1}(\omega)$ is the localization distance. The focus of our calculation is on the edge modes that occupy all, or part, of the common band gap of the two PHCs: $\omega_{\mathrm{lb}} < \omega < \omega_{\mathrm{ub}}$, where $\omega_{\mathrm{l(u)b}}$ are the lower (upper) band gap edges.

The radiated electric field is calculated by solving the wave equation in the frequency domain: $\nabla\times[\nabla\times\tilde{\mathbf{E}}(\mathbf{r},\omega)] = (\omega/c)^2\epsilon(\mathbf{r})\tilde{\mathbf{E}}(\mathbf{r},\omega) + i\omega\mu_0\tilde{\mathbf{J}}(\mathbf{r},\omega)$, where $\epsilon(\mathbf{r})$ represents the inhomogeneous dielectric permittivity of the entire structure, and $\tilde{\mathbf{J}}(\mathbf{r},\omega) = q\hat{r}_{\parallel}\delta^2(\hat{\mathbf{r}}_{\perp})\exp(i\omega r_{\parallel}/v)$ is the current density produced by the charge moving with the constant speed $\mathbf{v} = v\hat{r}_{\parallel}$ in the direction of $\hat{r}_{\parallel} = \mathbf{v}/v$, $r_{\parallel} = \mathbf{r}\cdot\hat{r}_{\parallel}$, and $\mathbf{r}_{\perp}\perp\hat{r}_{\parallel}$ are the two remaining spatial dimensions.

In the case of a continuous medium on both sides of the boundary, the TR problem has been solved [6,19] by stitching the analytically known solutions at the boundary. This approach is not workable in the case of PHCs because analytic solutions for the propagating waves cannot be obtained. However, the problem is simplified in the case of edge wave excitation due to the remaining periodicity in the x direction. Briefly, using the Bloch eigenmodes of the supercell as the expansion basis [34], the driven electric field can be expressed as an integral over the first Brillouin zone

$$\tilde{\mathbf{E}}(\mathbf{r},\omega) = q\sum_n \int_{\mathrm{BZ}} \frac{dk}{2\pi\epsilon_0}\frac{i\omega c_n(k,\omega)\mathbf{E}_{k,n}(\mathbf{r})}{(\omega+i\gamma)^2-\omega_n^2(k)}, \quad (1)$$

where the expansion coefficients $c_n(k,\omega)$ are given by an integral along the beam's path defined as $\mathbf{r} = r_{\parallel}\hat{r}_{\parallel}$:

$$c_n(k,\omega) = \int_{-\infty}^{\infty} dr_{\parallel}[\mathbf{u}_n^*(k,\mathbf{r})\cdot\hat{r}_{\parallel}]e^{i(\omega/v-k\cos\theta)r_{\parallel}}, \quad (2)$$

where θ is the angle between the directions of the beam's velocity and of the interface between the two PHCs. The summation over n includes all modes (edge and bulk), and an infinitesimal γ is introduced to ensure causality.

Only a discrete set of edge modes contributes to far-field radiation at frequencies inside the common bulk band gap, thus enabling the following asymptotic limit of Eq. (1) (see the Supplemental Material [27]) at $x \to +\infty$:

$$\mathbf{E}(\mathbf{r},t) \approx \sum_{m+}\int_{\omega_{\mathrm{lb}}}^{\omega_{\mathrm{ub}}} \frac{d\omega}{v_{m+}^{(g)}}\frac{qC_{m+}\mathbf{u}_{m+}}{4\pi\epsilon_0}e^{i(k_{m+}x-\omega t)}, \quad (3)$$

where $m+$ is the discrete index for all forward-propagating edge modes, with their corresponding wave numbers $\{k_{m+}(\omega)\}$ determined from the edge mode's dispersion relation $\omega_{m+}(k) = \omega$ and satisfying the causality condition $v_{m+}^{(g)}(\omega) \equiv (dk_{m+}/d\omega)^{-1} > 0$. The frequency-dependent spectral amplitudes $C_{m+}(\omega)$ of the transition edge radiation (TER) are obtained by substituting the implicitly frequency-dependent Bloch eigenfunctions $\mathbf{u}_{m+}(k_{m+},\mathbf{r})$ of the edge modes into Eq. (2): $C_{m+} \equiv c_{m+}[k_{m+}(\omega),\omega]$. The expression for the electric field propagating in the $x < 0$ direction is identical to Eq. (3), except that the contributing modes (labeled with $m-$ index) satisfy $v_{m-}^{(g)}(\omega) < 0$.

The power spectrum $P_{\pm}^{\mathrm{TER}}(\omega)$ of the forward or backward TER, which is finite for all frequencies where edge modes exist, can now be calculated (see the Supplemental Material [27]):

$$P_{\pm}^{\mathrm{TER}}(\omega) = \frac{q^2}{4\pi\epsilon_0}\sum_{m\pm}\frac{|C_{m\pm}|^2(\omega)}{v_{m\pm}^{(g)}(\omega)} \tag{4}$$

This intuitive expression for the spectral power of edge waves, which is applicable to both continuous (see the Supplemental Material [27] for the application of this formalism to SPP generation [6,19]) and photonic media, constitutes the main general result of this Letter.

Next, we consider a specific example of kink states' excitation at the domain wall between two topologically different PTIs shown in Fig. 2(a). The structure, based on Ref. [26], consists of two quantum spin-Hall (QSH) PTIs with opposite spin Chern numbers $C_s = \pm 1/2$. The QSH-PTIs are comprised of two parallel metal plates providing confinement in the z direction, patterned by a hexagonal lattice (of period a) arrangement of metal rods attached to either the top [right side of Fig. 2(a)] or the bottom (left side) metal plate. Its 1D-photonic band structure (PBS) and Bloch states are obtained using COMSOL eigenfrequency study. Figure 2(b) shows the PBS, where black dots denote bulk modes, and colored solid lines inside the band gap represent TPEWs.

The domain wall between two QSH-PTIs supports four TPEWs inside the band gap: two forward and two backward TPEWs (two at each valley). The group velocities of the TPEWs are locked to their photonic spin [26]: spin-up ($m+$, red lines) modes propagate forward, while spin-down ($m-$, green lines) modes propagate backwards. For our specific design, the TPEWs span the shared topological band gap bracketed by $\omega_{\mathrm{lb}} = 0.72(2\pi c/a)$ and $\omega_{\mathrm{ub}} = 0.77(2\pi c/a)$ from below and above, respectively. The TER-producing point charge is assumed to be moving along one of the high-symmetry axes of the hexagonal lattice, drawn through the midplane between the two metal plates and halfway between two adjacent rows of rods for optimal clearance. Therefore, the charge is crossing the domain wall between the two QSH-PTIs at the $\theta = \pi/3$ angle [see Fig. 2(a)], and is experiencing a periodic environment on both sides of the interface.

The choice of this specific photonic platform is dictated by its several unique properties. First, the supported TPEWs can be guided along sharply curved trajectories [22,24,26,35] after their excitation. Second, the specific geometry of QSH-PTIs is conducive to its interaction with high-power electromagnetic radiation. That is because the transverse confinement of the kink states does not require any side walls, and because the attachment of the rods to just one metal plate enables their easy monolithic fabrication. Third, the sparsity of the QSH-PTI structure and the existence of clear passages for the charged beam along multiple unobstructed directions prevent a direct impact of electrons on the structure. We note that it has been recently shown in theory that unidirectional edge states can be predominantly excited by Cherenkov emission using magnetized plasmas or Weyl semimetals [36].

The expression for the power spectrum $P_{\pm}^{\mathrm{TER}}(\omega)$ involves 4 TPEWs that are graphically shown as the crossing points between the yellow dashed (constant frequency) line and the dispersion relations (solid lines) of the TPEWs in Fig. 2(b). These crossings are labeled as

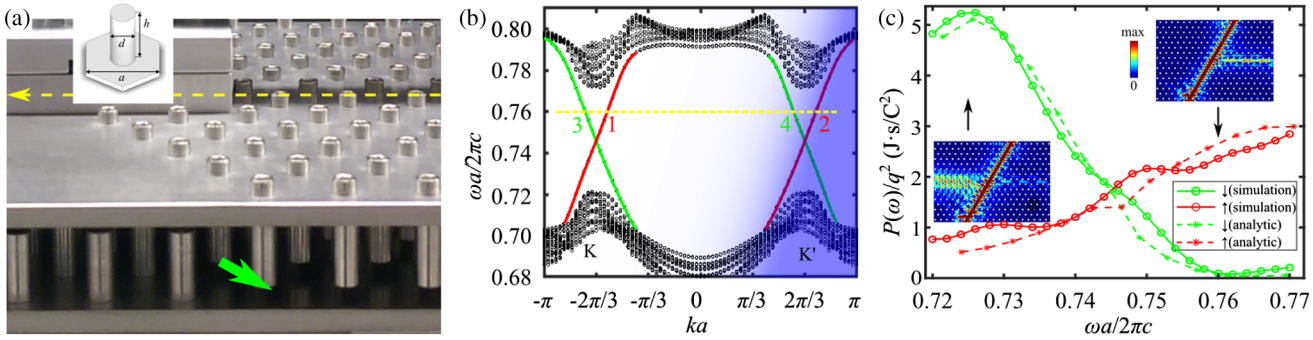

FIG. 2. (a) Fabricated photonic structure comprised of two QSH-PTIs separated by the domain wall. The charge travels in the midplane between the plates under the dashed yellow line. The spin-down waves (green arrow) will be received at one end of the interface (spin-up waves not shown). Inset: unit cell geometry with realistic dimensions: $a = 11.5$ mm, $d = 3.97$ mm, and $h = 9.78$ mm. (b) The 1D PBS of the structure, projected onto the x axis. Black dots: bulk modes continua separated by the band gap. Red (green) solid lines: TPEWs with up (down) (m_+/m_-) spins inside the band gap. Horizontal dashed line: constant-frequency line intersecting the four TPEWs at different values of $k_{m\pm}(\omega)$. Blue shaded area: the "strong excitation belt." (c) The emitted TER inside the band gap calculated from the analytic expression [Eq. (4), dashed lines] and *ab initio* simulation (solid lines). Red (green) lines: TER to the right (left) of the crossing point. Insets: the norm of the in-plane Poynting vector perpendicular to the beam's path $|S_\perp|$ obtained from the simulation, at frequencies labeled by the black arrows. The beam moves form the lower to the upper PTI domain, and its trajectory is covered by oversaturated red. The horizontal PTI interface is located in the middle of the plot, below (above) which rods are attached to the top (bottom) plate.

follows: $m = 1$, 2 crossings belong to $\{m+\}$ (spin-up TPEWs in the K/K' projected valleys), while $m = 3$, 4 correspond to their spin-down counterparts. The group velocities of all 4 TPEWs are approximately equal and constant across the band gap: $v_m^{(g)}(\omega) \approx 0.4c$. The predicted spectra are plotted in Fig. 2(c) for the right- (left-)propagating TPEWs [dashed red (green) lines], and are found in good agreement with *ab initio* driven simulation (solid lines), where $\tilde{\mathbf{J}}(\mathbf{r}, \omega)$ is implemented as the current source.

The TER spectra exhibit several notable features. First, we find that TER can be highly directional and spin-polarized: see the insets in Fig. 2(c) corresponding to $\omega_\downarrow \approx 0.725(2\pi c/a)$ (predominantly backward spin-down radiation), and to $\omega_\uparrow \approx 0.76(2\pi c/a)$ (forward spin-up radiation). On the other hand, for other frequencies at the center of the band gap both forward and backward TPEWs of similar intensities are launched. Second, excitation of K valley TPEWs ($m = 1$, 3) is negligible compared with excitation of their K' valley ($m = 2$, 4) counterparts (see Fig. S2 in Supplemental Material [27] for the spectra of all 4 TPEWs). Therefore, transition radiation mechanism provides a new way of valley-polarized excitation of TPEWs, and provides an opportunity to introduce the concept of quasiphase matching (QPM) between charges and radiation.

The essence of QPM is that under the envelope function approximation [37], TPEWs are constructed from bulk modes of the 2D-periodic PHC with imaginary k_y^{bulk} (for the QSH-PTI we used, the edge mode with 1D wave vector k is constructed from bulk modes with purely imaginary $k_y^{\text{bulk}} = \pm i\kappa \approx \pm 0.38 i a^{-1}$ and real $k_x^{\text{bulk}} = k \pm 2\pi/a$ for $K(k < 0)$ and $K'(k > 0)$ valley, respectively, due to band folding [38]), and for weakly confined TPEWs, the projection of the real part of the 2D wave vector $\mathbf{k}^{\text{bulk}}$ onto the charge trajectory must approximately match the wave number ω/v of the line current (or differ by a reciprocal vector) in order to get large overlap integral Eq. (2). Quantitatively, strong excitation of an edge mode is possible when its ω and k_x^{bulk} satisfies

$$|\omega/v - k_x^{\text{bulk}} \cos\theta + 2\pi N/a'| \lesssim \kappa \sin\theta, \tag{5}$$

for some integer N, where a' is the period along the beam's path. Note that in the limit of $\kappa \sin\theta \to 0$, we recover the so-called generalized Cherenkov condition [39]. We refer to the region defined by Eq. (5) as "strong excitation belt," and it is graphically represented in Fig. 2(b) as the blue shaded area ($N = -1$ for K' valley and $a' = a$). It's clear that only TPEWs at K' valley fall into this belt, and this explains why they are predominantly excited. One can also see the reason why the backward-moving TPEW 4 is excited much stronger at the lower edge of the band gap than at the upper edge: its dispersion line lies deep inside the belt at lower frequencies but outside at higher frequencies. Additional examples corresponding to a subrelativistic beam with $v = 0.56c$ (strong excitation belt covering K valley modes) and $v = 0.75c$ (no excitation), as well as detailed derivation of Eq. (5) are presented in the Supplemental Material [27]. The total emitted energy in the topological band gap vs v is also plotted, where multiple sharp peaks correspond to significantly enhanced TER when the QPM condition is satisfied. QPM is important when (i) the edge mode can be well described by decaying bulk modes and (ii) the wave decay constant κ satisfies $\kappa a' \sin\theta \ll 2\pi$. Note that, formally, the QPM condition resembles the relationship between the emission angle θ and the frequency ω of the Smith-Purcell radiation produced by a charge moving along a periodic structure [40,41]. The key differences in the case of TER considered by us are as follows: (i) radiation is coupled into a discrete set of edge states, not into a bulk continuum, (ii) the emission angle θ is fixed by the relative orientations of the charge trajectory and the interface, and (iii) due to the transient nature of TER, the QPM condition is an inequality rather than a strict equation.

The experimental validation of the TER concept was carried out at the Argonne Wakefield Accelerator Facility (AWA-ANL) using a high-charge relativistic pointlike electron beam ($q \sim 3$ nC, $E_b \approx 65$ Mev, and $\tau_b \approx 3$ ps) and a photonic structure that was modeled above. As sketched in Fig. 2(a), the bunch (yellow dashed line) traverses the interface between the two QSH-PTI domains near the center of the structure and excites TPEWs around the frequency of $f_0 \equiv \omega_0/2\pi \approx 19.5$ GHz. The fully assembled structure is pictured in Fig. 3(a) inside a vacuum chamber. The objectives were to experimentally demonstrate the following: (a) unobstructed charged bunch propagation over many periods of the PHC along one of its principal directions under full vacuum, (b) the capability of the TR mechanism to exciting TPEWs inside the bulk band gap, and (c) spatial localization of TPEWs close to the domain wall. The PHC was comprised of 15×13 unit cells, and its dimensions listed in the caption of Fig. 2

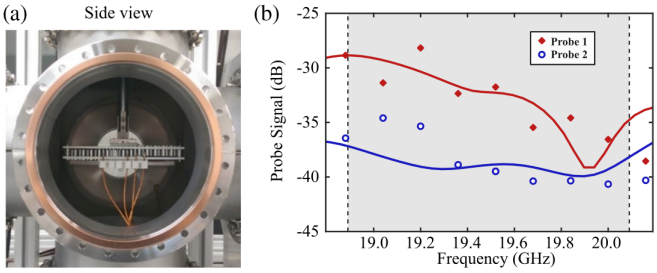

FIG. 3. Experimental demonstration of transition edge-wave radiation (TER) using two interfaced QSH-PTIs. (a) fabricated structure inside the chamber. (b) Experimentally measured signals by Probe 1 (red diamonds) and 2 (blue circles). Numerical prediction: solid red (blue) curves for Probe 1 (2). Shadowed area: photonic band gap, where only TPEWs exist.

ensure a topological PBG in the $19 < f < 20$ GHz range (where $f = \omega/2\pi$).

For diagnosing the TER produced by the bunch, two probes were positioned along the outer edge of the structure to detect spin-down waves: one very close (Probe 1), the other (Probe 2) six periods away from the interface (see the Supplemental Material [27] for their exact positions). The comparison between the signals from the two probes [see Fig. 3(b)] is used to demonstrate spatial localization of the EM energy at the interface. Indeed, the measured signal from Probe 1 (red diamonds) is much stronger that from Probe 2 (blue circles) for every frequency inside the PBG (shadowed area). This contrast, which approaches 10 dB for some of the frequencies, implies that the beam excites edge waves. Topological protection of such modes has been demonstrated earlier [24] using antenna excitation. To our knowledge, this is the first time that TPEWs were shown to be excited via the TR mechanism. Due to the limitation of the present experimental setup, we were only able to reliably measure signals at one end of the interface. Nonetheless, the measured result captures the most salient features predicted by our theory. For example, we see a clear trend of the TER decreasing in power as the frequency increases from the lower to the upper edge of the PBG. This is a consequence of the breakdown of the QPM near the upper edge of the PBG, as predicted by numerical simulation (solid red curve) and discussed above. Although the CR produced by the beam outside of the band gap is beyond the scope of this Letter, we note that the frequency positions (at 16 GHz and 18 GHz) of its two measured spectral peaks are also in good agreement with simulations results. Additional experimental and data processing details can be found in the Supplemental Material [27]. Future improvement of the experiment includes measuring spin-down waves and using a long train of electron bunches.

The TER concept can be used for beam diagnostics in the same way as TR of bulk waves because $P_{\pm}^{\mathrm{TER}}(\omega)$ strongly depends on the beam's energy, duration, and the location of its trajectory. Novel beam-driven accelerators, such as matrix [42] and two-beam accelerators (TBAs) [43], and accelerators with a photonic-band-gap structure [44] can also benefit from TER. For example, possible geometries of a TER-based noncollinear (but parallel) TBA and a matrix accelerator are shown in Supplemental Material [27].

This work was supported by the Army Research Office (ARO) under Grant No. W911NF-16-1-0319, and by the U.S. Department of Energy (DOE) Office of Science under Grant No. DE-SC0007889.

*gshvets@cornell.edu

[1] P. A. Cherenkov, Dokl. Akad. Nauk SSSR **2**, 457 (1934).
[2] I. M. Frank and V. L. Ginzburg, J. Phys. (Moscow) **9**, 353 (1945).
[3] M. L. Ter-Mikaielian, *High Energy Electromagnetic Processes in Condensed Media* (Wiley, New York, 1972).
[4] J. M. Frank, Acta Phys. Pol. A **38**, 655 (1970).
[5] G. M. Garibian, in *Proc. Conf. High Energy Physics Instrumentation* (Dubna, 1970), Vol. 2, p. 509.
[6] V. Ginzburg and V. Tsytovich, *Transition Radiation and Transition Scattering* (Adam Hilger, Bristol and New York, 1990).
[7] U. Happek, A. J. Sievers, and E. B. Blum, Phys. Rev. Lett. **67**, 2962 (1991).
[8] M. L. Cherry, G. Hartmann, D. Müller, and T. A. Prince, Phys. Rev. D **10**, 3594 (1974).
[9] L. Wartski, S. Roland, J. Lasalle, M. Bolore, and G. Filippi, J. Appl. Phys. **46**, 3644 (1975).
[10] G. Adamo, J.-Y. Ou, J. K. So, S. D. Jenkins, F. De Angelis, K. F. MacDonald, E. Di Fabrizio, J. Ruostekoski, and N. I. Zheludev, Phys. Rev. Lett. **109**, 217401 (2012).
[11] X. Artru, G. B. Yodh, and G. Mennessier, Phys. Rev. D **12**, 1289 (1975).
[12] B. Pardo and J.-M. André, Phys. Rev. A **40**, 1918 (1989).
[13] M. A. Piestrup and P. F. Finman, IEEE J. Quantum Electron. **19**, 357 (1983).
[14] G. Bekefi, J. S. Wurtele, and I. H. Deutsch, Phys. Rev. A **34**, 1228 (1986).
[15] X. Lin, S. Easo, Y. Shen, H. Chen, B. Zhang, J. D. Joannopoulos, M. Soljačić, and I. Kaminer, Nat. Phys. **14**, 816 (2018).
[16] M. Kuttge, E. J. R. Vesseur, A. F. Koenderink, H. J. Lezec, H. A. Atwater, F. J. G. de Abajo, and A. Polman, Phys. Rev. B **79**, 113405 (2009).
[17] C. Chen and J. Silcox, Phys. Rev. Lett. **35**, 389 (1975).
[18] A. Yurtsever, M. Couillard, and D. A. Muller, Phys. Rev. Lett. **100**, 217402 (2008).
[19] F. J. Garciade Abajo, Rev. Mod. Phys. **82**, 209 (2010).
[20] G. Wilson, J. R. Dennison, A. E. Jensen, and J. Dekany, IEEE Trans. Plasma Sci. **41**, 3536 (2013).
[21] M. Hafezi, E. A. Demler, M. D. Lukin, and J. M. Taylor, Nat. Phys. **7**, 907 (2011).
[22] A. B. Khanikaev, S. H. Mousavi, W.-K. Tse, M. Kargarian, A. H. MacDonald, and G. Shvets, Nat. Mater. **12**, 233 (2013).
[23] M. Hafezi, S. Mittal, J. Fan, A. Migdall, and J. Taylor, Nat. Photonics **7**, 1001 (2013).
[24] K. Lai, T. Ma, X. Bo, S. Anlage, and G. Shvets, Sci. Rep. **6**, 28453 (2016).
[25] H. Soifer, A. Gauthier, A. F. Kemper, C. R. Rotundu, S. Yang, H. Xiong, D. Lu, M. Hashimoto, P. S. Kirchmann, J. A. Sobota *et al.*, Phys. Rev. Lett. **122**, 167401 (2019).
[26] T. Ma, A. B. Khanikaev, S. H. Mousavi, and G. Shvets, Phys. Rev. Lett. **114**, 127401 (2015).
[27] See Supplemental Material at http://link.aps.org/supplemental/10.1103/PhysRevLett.123.057402 for alternative configurations, which includes Refs. [28–32].
[28] G. W. Ford and W. H. Weber, Phys. Rep. **113**, 195 (1984).
[29] M. Wada, S. Murakami, F. Freimuth, and G. Bihlmayer, Phys. Rev. B **83**, 121310(R) (2011).
[30] S. E. Tsimring, *Electron beams and microwave vacuum electronics* (John Wiley and Sons, Inc., Hoboken, New Jersey, 2007).

[31] D. M. Goebel, J. M. Butler, R. W. Schumacher, J. Santoru, and R. L. Eisenhart, IEEE Trans. Plasma Sci. **22**, 547 (1994).
[32] M. A. Shapiro, S. Trendafilov, Y. Urzhumov, A. Al'u, R. J. Temkin, and G. Shvets, Phys. Rev. B **86**, 085132 (2012).
[33] J. D. Joannopoulos, S. G. Johnson, J. N. Winn, and R. D. Meade, *Photonic Crystals: Molding the Flow of Light*, 2nd ed. (Princeton University Press, Princeton and Oxford, 2008).
[34] K. Sakoda, *Optical Properties of Photonic Crystals* (Springer-Verlag, Berlin Heidelberg, 2005).
[35] W.-J. Chen, S.-J. Jiang, X.-D. Chen, B. Zhu, L. Zhou, J.-W. Dong, and C. T. Chan, Nat. Commun. **5**, 5782 (2014).
[36] F. R. Prudêncio and M. G. Silveirinha, Phys. Rev. B **98**, 115136 (2018).
[37] G. Bastard, *Wave Mechanics Applied to Semiconductor Heterostructures*, Monographies de Physique (Les Éditions de Physique, Les Ulis, 1988).
[38] T. Ma and G. Shvets, New J. Phys. **18**, 025012 (2016).
[39] C. Kremers, D. N. Chigrin, and J. Kroha, Phys. Rev. A **79**, 013829 (2009).
[40] N. Yamamoto, F. Javier Garciade Abajo, and V. Myroshnychenko, Phys. Rev. B **91**, 125144 (2015).
[41] I. Kaminer, S. E. Kooi, R. Shiloh, B. Zhen, Y. Shen, J. J. López, R. Remez, S. A. Skirlo, Y. Yang, J. D. Joannopoulos, A. Arie, and M. Soljacic, Phys. Rev. X **7**, 011003 (2017).
[42] D. H. Whittum and S. G. Tantawi, Rev. Sci. Instrum. **72**, 73 (2001).
[43] S. Y. Kazakov, S. V. Kuzikov, Y. Jiang, and J. L. Hirshfield, Phys. Rev. ST Accel. Beams **13**, 071303 (2010).
[44] E. I. Smirnova, A. S. Kesar, I. Mastovsky, M. A. Shapiro, and R. J. Temkin, Phys. Rev. Lett. **95**, 074801 (2005).